has some notion of the associated collective mode (by which we mean that coherent part of the motion which effects a strong feedback via the self-consistent field). For example, the picture of the $\Delta T=1$ collective dipole vibration, as one in which neutron and proton densities move through one another as hard spheres, suggests the interaction

$$V(1,2)=-g\sum_{\mu}\tau_0(1)\frac{du_0}{dr}(r_1)Y_{1\mu}^*(\theta_1)\tau_0(2)\frac{du_0}{dr}(r_2)Y_{1\mu}(\theta_2).$$

But again this interaction does not imply that the normal modes actually are the simple collective mode pictured. The assumption is that only this collective component of the normal-mode motion effects any substantial feedback on the self-consistent field.

ACKNOWLEDGMENTS

The author would like to thank Professor G. E. Brown for stimulating criticism and Professor S. A. Moszkowski for helpful discussions and for bringing to his attention a similar basis for the SDI.[20]

[20] S. A. Moszkowski, in Proceedings of the International Conference on Nuclear Structure, Gatlinburg, Tennessee, 1966 (to be published).

PHYSICAL REVIEW VOLUME 162, NUMBER 4 20 OCTOBER 1967

Polarization in p-α Scattering*

M. F. JAHNS† AND E. M. BERNSTEIN
Department of Physics, The University of Texas, Austin, Texas
(Received 5 June 1967)

The polarization of protons elastically scattered from ^{4}He was measured at a total of 11 points including six different angles and four energies between 6 and 11 MeV. Carbon was used as an analyzer. Excellent agreement was obtained between the present results and the measurements of Brown, Haeberli, and Saladin. A phase-shift analysis at 10 MeV provides evidence for small positive split d waves at this energy with the $d_{5/2}$ phase shift 1 to 2 deg larger than the $d_{3/2}$ phase shift.

I. INTRODUCTION

THE possibility of producing polarized nucleons by elastic scattering was suggested by Schwinger[1,2] in 1946. Schwinger suggested that nucleons scattered from ^{4}He might be polarized, since a low-lying resonance level in ^{5}Li was thought to be split by spin-orbit coupling. The polarization of protons scattered elastically from helium was first measured in 1951 by Heusenkveld and Freier[3] at the University of Minnesota. An analysis of these results used in conjunction with a phase-shift analysis by Critchfield and Dodder[4] of differential cross-section measurements for ^{4}He$(p,p)^4$He scattering in the region of 1–4 MeV gave conclusive evidence that the $P_{1/2}$ and $P_{3/2}$ energy levels in the ^{5}Li* compound nucleus are inverted. Further measurements by Juveland and Jentschke[5] in 1956 and by Rosen and Brolley[6] in 1957 determined that the polarization of protons scattered from helium was quite high for proton energies up to 10 MeV and that helium could therefore be used as a polarization analyzer for protons of energy up to 10 MeV resulting from other reactions. In 1957, Brockman[7] used helium as a polarization analyzer to measure the polarization of 17.7-MeV protons scattered from five other elements.

Since that time, many experiments have been carried out in which ^{4}He$(p,p)^4$He scattering was used either as a source of polarized protons or to analyze the scattering from another element.

For the 17.7-MeV polarization measurements by Brockman, [7] the polarization-analyzing power of helium as a function of energy and angle was calculated from phase shifts had been determined by an analysis of differential cross-section measurements of ^{4}He$(p,p)^4$He scattering. Since phase shifts derived in this manner are not always unique, and since the cross section is not as sensitive as the polarization to small changes in phase shifts, polarizations calculated in this manner are not too reliable. Therefore, much interest has been given to the direct measurement of proton polarization in ^{4}He$(p,p)^4$He scattering.

Brown, Haeberli, and Saladin[8] have recently measured the proton polarization in ^{4}He$(p,p)^4$He by double scattering from helium at laboratory angles of 45.8°,

* Work supported in part by the U. S. Atomic Energy Commission.
† National Aeronautics and Space Administration Fellow; Present Address: Sam Houston State College, Huntsville, Texas.
[1] J. Schwinger, Phys. Rev. **69**, 681 (1946).
[2] J. Schwinger, Phys. Rev. **73**, 407 (1948).
[3] M. Heusenkfeld and G. Freier, Phys. Rev. **85**, 80 (1952).
[4] C. L. Critchfield and D. C. Dodder, Phys. Rev. **76**, 602 (1949).
[5] A. E. Juveland and W. Jentschke, Z. Physik **144**, 521 (1956).
[6] L. Rosen and J. E. Brolley, Jr., Phys. Rev. **107**, 1454 (1957).
[7] K. W. Brockman, Jr., Phys. Rev. **110**, 163 (1958).
[8] R. Brown, W. Haeberli, and J. X. Saladin, Nucl. Phys. **47**, 212 (1963).

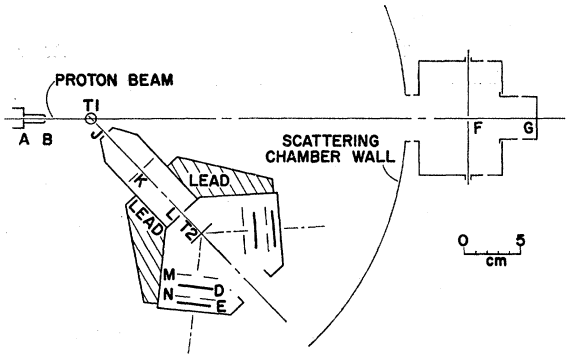

FIG. 1. Top view of double-scattering apparatus. The figure is schematic but to scale. Slits B and K shield the first and second targets from particles scattered from the apparatus. The distance between the 1st and 2nd targets is 15.29 cm. Other pertinent dimensions are given in Table I.

60.8°, 75.6°, and 115.1° for incident proton energies near 4.7, 5.9, 7.9, 9.9, and 11.9 MeV. The results of these measurements indicated that the polarization predicted by the best available sets of phase shifts[7] are in error by as much as 0.08.

In the present experiment, the polarization of protons scattered elastically from ^{4}He was measured at a total of 11 points, including four different energies and six different laboratory angles. The polarization was analyzed by a second scattering from a carbon-foil target. Energies and angles in the first scattering were chosen such that these polarization measurements could advantageously be combined with the polarization measurements of Brown *et al.*,[8] and with the ^{4}He$(p,p)^4$He cross-section measurements of Barnard *et al.*,[9] in order to make a phase-shift analysis.

The results of the polarization measurements are given in Sec. V. The results of the phase-shift analysis are given in Sec. VI.

TABLE I. Dimensions of the defining apertures.

Aperture system	Designation (Fig. 2)	Aperture size, mm, diameter or width × height	Distance from given location, cm (Fig. 2)
Incident beam	B	2.03 × 3.30	4.13 from T1
	A	1.27 × 2.54	6.03 from T1
	Not shown	4.77	34.5 from T1
Between first and second target	J	2.16[a] × 15.87	1.867 from T1
	K	6.65 × 15.09	6.350 from T1
	L	4.77 × 20.47	11.748 from T1
Between second target and detector	M	9.98 × 26.97	3.810 from T2
	N	6.12 × 15.87	5.682 from T2
Beam monitoring	F	2.39 width	36.1 from T1

[a] For first scattering angles of 60° or larger, the width of this slit was 4.17 mm.

[9] A. C. L. Barnard, C. J. Jones, and J. L. Weil, Nucl. Phys. **50**, 604 (1964).

II. APPARATUS

The apparatus for this experiment was designed to use helium gas as a first target and a self-supporting carbon foil as a second target. The twice-scattered protons were detected by two counter telescopes, each of which consisted of a surface-barrier detector located behind a totally depleted ΔE detector. Energy-absorbing foils were placed between the first and second targets to lower the proton energies to desired values. Coincidence counts from the two telescopes were recorded simultaneously in two 100-channel sections of a 400-channel analyzer.

A simplified top view of the scattering equipment is shown in Fig. 1. The proton beam from The University of Texas tandem accelerator was defined by slit A and a circular aperture located 34.5 cm to the left of the first target. Important dimensions of these and other apertures are given in Table I. The rear slits F and the beam stop G were electrically insulated from the ground and from each other to allow the current to be integrated and also to determine that the beam was passing through the center line of the apparatus.

Protons scattered from the gas target cell T1 (see Fig. 1) through an angle θ_1 pass through the first scattering aperture system consisting of slits J, K, and L, and reach the carbon foil target T2. K is an anti-scattering slit. Polyethylene and aluminum foils were inserted in front of slit K during some of the measurements to lower the energy of protons reaching the second target.

Protons scattered from the second target through an angle θ_2 travel through the second scattering slit system (consisting of slits M and N), through the right ΔE detector D, and into the right energy detector E. Protons scattered through an angle $-\theta_2$ will similarly be detected by the left counter telescope. The entire assembly, consisting of the first scattering slit system, the second target, the second scattering slit system, and the detectors, may be rotated within the scattering chamber so that the first scattering angle θ_1 may be varied continuously from ±35° to ±135°.

The aperture locations and sizes are a compromise of features that give a reasonable counting rate and also allow geometrical corrections to be made quite accurately.

The alignment of the double-scattering apparatus with respect to the scattering chamber was determined with an alignment telescope.[10] The components of the beam-collimating system were fabricated and assembled to tolerances of 0.025 mm. Monitoring the beam current on the rear slits F (Fig. 1) insured that the beam passed through the scattering chamber at 0° to within ±0.1°. The first scattering angle could be set to within ±0.05°.

[10] Alignment telescope manufactured by Taylor, Taylor, and Hobson, Leicester, England, available in the U. S. A. from Engis Equipment Company, Chicago, Illinois.

TABLE II. Measured values of R and P_2^{eff} obtained from double scattering of protons from carbon. Energies and angles are in the laboratory system. The thickness of the second target is ΔE_2.

E_1 (MeV)	θ_1 (deg)	E_2 (MeV)	ΔE_2 (keV)	θ_2 (deg)	R	P_1[a]	P_2^{eff}
5.637	50	5.072	218	50	5.354±0.135	−0.868±0.022	−0.813±0.022
6.230	50	5.650	200	50	3.604±0.085	−0.692±0.013	−0.849±0.020
7.180	70	5.810	198	50	0.182±0.009	+0.856±0.018	−0.842±0.023
7.180	70	6.035	190	50	0.243±0.010	+0.856±0.018	−0.747±0.025
7.180	70	6.242	186	50	0.300±0.013	+0.856±0.018	−0.661±0.025

[a] See Ref. 15.

The components of the first scattering aperture system were located to within 0.025 mm of the values shown in Table I, insuring that the centerline through the apertures was within 0.03° of the desired direction. It was also verified that this centerline passed through the center rotation to within 0.040 mm.

The centerlines of the second scattering aperture system were located at ±(50.00±0.05)° with respect to the first scattering centerline, and the detector apertures defined equal acceptance solid angles about the center of the second target to within ±0.7%.

Right-left intensity ratios were measured alternately on the right and left sides of the beam to obtain cancellation of false asymmetries from certain types of instrumental misalignments. The right-to-left ratio was taken to be the geometric mean of the two values.[11] It is estimated that the greatest uncertainty in the asymmetry resulting from possible misalignment is less than 0.007.

The design of the gas targets used in this experiment is essentially a copy of the cells used by Brown *et al.*[8] Helium gas of 99.99% minimum purity at a pressure of 10 atm (absolute) was contained within a 0.95-cm-diam cylinder. The walls of the cylinder were fabricated of 4.1-μm Havar[12] foil glued with an epoxy resin.[13]

The purity of the helium gas used was checked by observing the energy distribution of single-scattered protons with a surface-barrier detector. The number of protons scattered by contaminants was less than 0.1% of the number scattered by helium. If the polarizing power of the contaminants were 100% in the sense opposite that of helium, these contaminants could cause an error of not more than 0.002 in the asymmetries measured. The beam current incident upon the gas cell varied from 1.2 μA at 6 MeV to 2.2 μA at 11 MeV.

The carbon-foil target used as the polarization analyzer in this experiment was prepared by allowing a layer of Alcohol-Dag,[14] a colloidal suspension of carbon in alcohol, to dry on a glass slide. A carbon foil of 3.47-mg/cm^2 thickness was used for all measurements.

The purity of the carbon-foil target was investigated by observing the energy distribution of single-scattered protons with a surface-barrier detector. This spectrum showed the target foil to contain a small oxygen contaminant in an amount similar to that found in foils used in previous carbon-polarization investigations by Terrell *et al.*[15] The effective analyzing power for the particular carbon foil used was accurately determined in this experiment, so that the presence of a small amount of oxygen had no undesirable effect.

III. EXPERIMENTAL PROCEDURE

To measure the polarization of helium at the desired angles and energies, it was necessary to determine accurately the effective analyzing power of the carbon-foil second target. This was accomplished by making a series of measurements of the right-left intensity ratios using a carbon-foil first target for which the polarizing power had been determined. The analyzing target used in these measurements was the same 3.47-mg/cm^2 carbon foil which was used in all the helium measurements of this experiment. The polarizing power of the 2.65-mg/cm^2 carbon foil used as the first target had previously been determined by Terrell *et al.*,[15] using the method of Scott and Segel.[16,17]

The number and duration of runs for each measurement were sufficient to provide a statistical uncertainty in the asymmetry comparable to the total uncertainty in the known values of the polarizing power of the first target. During these measurements, the first target was rotated between runs in order to cancel any effect of the first target plane not being coincident with the center of rotation.

Table II gives the geometric mean right-left counting ratios R measured for carbon-carbon scattering and their statistical uncertainties. Also listed in Table II are the values of the polarizing power P_1 and the calculated values of the effective polarization for the analyzing target P_2^{eff}. The uncertainty shown for P_1 is the total uncertainty. The statistical uncertainty is

[11] I. Alexeff and W. Haeberli, Nucl. Phys. **15**, 609 (1960).

[12] Havar is the trade name of a high tensile strength cobalt base alloy manufactured by the Precision Metals Division of Hamilton Watch Company, Lancaster, Pennsylvania.

[13] Armstrong A-4, supplied by Armstrong Products, Warsaw, Illinois.

[14] Dispersion No. 154, supplied by Acheson Colloids Company, Port Huron, Michigan.

[15] G. E. Terrell, M. R. Kostoff, M. F. Jahns, and E. M. Bernstein, Bull. Am. Phys. Soc. **10**, 103 (1965); (private communication).

[16] M. J. Scott and R. E. Segel, Bull. Am. Phys. Soc. **30**, 16 (1955).

[17] M. J. Scott, Phys. Rev. **110**, 1398 (1958).

TABLE III. Intensity ratios and corresponding angles and energies for the ^{4}He measurements. Energies and angles are in the laboratory system.

No.	E_1 (MeV)	θ_1 (deg)	E_2 (MeV)	θ_2 (deg)	R
1	6.000	37.7	5.072	50	1.701±0.028
2	7.891	37.7	6.160	50	1.693±0.024
3	7.891	45.5	5.589	50	2.157±0.044
4	7.891	45.5	6.171	50	1.905±0.047
5	7.891	45.5	6.171	50	1.888±0.034
6	7.891	45.5	6.178	50	2.058±0.052
7	9.890	36.0	6.075	50	1.556±0.036
8	9.890	37.7	5.962	50	1.615±0.039
9	9.890	45.5	5.933	50	1.925±0.045
10	9.890	45.5	6.062	50	1.809±0.033
11	9.890	60.8	5.863	50	2.795±0.070
12	9.890	60.8	6.114	50	2.442±0.077
13	9.890	60.8	6.114	50	2.593±0.086
14	9'890	75.6	6.185	50	2.960±0.114
15	9.890	85.3	5.617	50	2.856±0.166
16	9.890	85.3	5.877	50	2.685±0.119
17	9.890	100.0	5.076	50	0.438±0.031
18	9.890	100.0	5.076	50	0.460±0.026
19	11.156	85.3	6.213	50	2.057±0.118
20	11.156	100.0	5.797	50	0.450±0.030

shown for P_2^{eff}. The direction of positive polarization is $\mathbf{k}_{\text{in}}\times\mathbf{k}_{\text{out}}$ (Basel convention).

The value of P_2^{eff} were computed from the measured ratios by an electronic computer in the manner discussed in Sec. IV. In addition to the results of Terrell *et al.*,[15] the results of Moss and Haeberli[18] and Nikolic *et al.*[19] were used in calculating polarization and cross-section derivatives required for geometry corrections.

The energy spread due to the second target thickness is listed as $\Delta E2$. In determining the total uncertainty in the final results for the helium measurements, an uncertainty in P_2 due to the uncertainty in the second scattering energy E_2 was included. The uncertainty in E_2 was of the order of 35 keV.

The difference between $P_2^{\text{eff}}(E,\theta)$ and the actual $P(E,\theta)$ for carbon is due to the small oxygen contamination in the target foil used. Estimated corrections to P_2^{eff} give values in agreement with the values of carbon polarization measured by Terrell *et al.*[15] and by Moss and Haeberli.[18]

The polarization of protons scattered from ^{4}He was measured at a total of 11 points, including four different energies and six different laboratory angles. The geometrical mean of the right-left counting ratio R measured for these points is given in Table III. The uncertainties in R given are statistical uncertainties combined with uncertainties in background correction.

In several cases, the polarization of protons scattered from helium at a given energy and angle was measured using various analyzer scattering energies E_2. In addition to obtaining smaller statistical errors by these additional runs, statistically consistent results indicated that no significant error had been made in calculating energy losses in foils, absorbers, etc.

The right-left counting ratio for individual runs of a measurement were always within a standard deviation of the geometrical mean for that measurement.

For first scattering energies E_1 of 6.00 and 7.89 MeV, the background counting rate was so low that it could be neglected in every measurement. At 9.89 and 11.16 MeV, background measurements were necessary at $\theta_1=85.3°$ and 100° (lab angles). Although background counts could be seen in the spectra at more forward angles at 9.89 MeV, the greater energy of protons scattered at smaller angles permitted a higher analyzer energy E_2 to be used. The energy of the twice-scattered protons was then such that the foreground pulses could be resolved from the background. The average background for the two energies and two angles stated above was 4% of the foreground counting rate.

Background was measured by replacing the carbon-foil target with a bare target frame. The gas cell first target was not removed because it appeared that part of the background was caused by a reaction of protons with some element in the Havar foil of the gas cell.

Runs to determine background counting rates were in general of shorter duration than foreground runs. Since the current integrator measured the beam which struck the beam stop G at the rear of the scattering chamber (Fig. 1) but did not include that which struck the monitoring slits F, an additional uncertainty was introduced into the background corrections. The uncertainty in the background resulting from this effect was assumed to be 15%. The rms of this uncertainty, the statistical uncertainty in the background, and the statistical uncertainty in the foreground, were used as the statistical uncertainty in the counting rate.

IV. CALCULATION OF ASYMMETRIES AND GEOMETRY CORRECTIONS

The counting rate dI for an infinitesimal detector counting particles doubly scattered from infinitesimal first and second targets is given by

$$dI^{\pm}=K\sigma_1(E_1,\theta_1)d\Omega_1\sigma_2(E_2,\theta_2)\times d\Omega_2{}^{\pm}[1+P_1(E_1,\theta_1)A_2(E_2,\theta_2)\cos\phi^{\pm}]. \quad (1)$$

The plus or minus sign indicates that the first and second scattering angles, θ_1 and θ_2, are both in the same or in an opposite sense, respectively. The K appearing in Eq. (1) is a factor determined by the beam current and by the thickness of the first and second targets. σ_1 and $d\Omega_1$ are the cross section and solid angle, respectively, for the first scattering which occurs at an energy E_1. Similar definitions hold for σ_2 and $d\Omega_2$. The quantity P_1 is the polarization effected by the first scattering, and $A_2(E_2,\theta_2)$ is the analyzing power of the second target for incident particles of energy E_2 scattered at an angle θ_2. For elastic scattering, $A_2=P_2$ for

[18] S. J. Moss and W. Haeberli, Nucl. Phys. **72**, 417 (1965).
[19] N. Nikolic, L. J. Lidofsky, and T. H. Kruse, Phys. Rev. **132**, 2212 (1963).

the same center-of-mass angle and energy. Cosϕ is the cosine of the angle between the normals to the two scattering planes.

To determine the counting rate for a finite apparatus, Eq. (1) should be integrated over the limits of scattering angles and energies determined by target thicknesses and aperture sizes. Since the energies and angles involved in Eq. (1) can be expressed in terms of the spatial coordinates describing a double-scattering event, the integration indicated above can in principle be carried out if the functional forms of σ_1, σ_2, P_1, and P_2 are known.

In order to carry out the indicated calculation, each cross section and polarization involved in a particular event was expanded in a Taylor series as a function of the scattering angle and energy. The expansion was made about the angle and energy an event would have if it occurred along the centerlines of the geometry. The targets and detector surfaces were then divided into adequately small subdivisions and Eq. (1) was integrated for the entire geometry by numerical integration.

The Taylor expansion for the polarization of the first scattering is, for example,

$$P_1(E_1,\theta_1)=P_1(E_{10},\theta_{10})[1+P_1'_{E_0}(E_1-E_{10}) +P_1'_{\theta_0}(\theta_1-\theta_{10})+\tfrac{1}{2}P_1''_{\theta_0}(\theta_1-\theta_{10})^2]. \quad (2)$$

The zero subscripts, i.e., E_{10}, θ_{10}, etc., refer to energies and angles of events which occur at the center of targets and detector surfaces. $P_1'_{E_0}$ is the logarithmic derivative of the polarization with respect to energy, evaluated at E_0, etc. Investigation showed that derivatives of higher order than those shown in Eq. (2) may be neglected in the present case.

It was assumed in the calculations that the scattering volume within the gas target cell could be approximated by a line along the direction of the beam. In the numerical integration, this line was subdivided into line segments sufficiently small so that each segment could be treated as a point. The carbon-foil second target was assumed to be a plane and was subdivided into meshes small enough so that each mesh could be treated as a point. The surfaces of the energy detectors were subdivided in a similar manner.

The total counting rate for finite first and second targets and detectors is obtained by substituting the Taylor expansions for the cross sections and polarizations into Eq. (1) and integrating over the limits determined by the apparatus. The numerical integration was performed using the University of Texas CDC 1604 electronic computer.

The calculation described above requires a knowledge of the energy and angular dependence of the ^{4}He$(p,p)^4$He cross sections and polarizations in order to determine the derivatives entering expressions of the form of Eq. (2). However, the derivatives need to be known only approximately, since the geometry corrections are rather small. Good values for the cross-section derivatives were obtained from the cross-section measurements of Barnard *et al.*[9] The polarization derivatives were obtained using the measurements of Brown *et al.*,[8] the uncorrected data of the present experiment, and the predicted polarizations given in Ref. 9. After the geometry corrections to the present data were made, it was verified that the polarization derivatives used for the corrections were satisfactory.

TABLE IV. Asymmetries P_1P_2 for protons doubly scattered from ^{4}He and carbon. Energies and angles are in the laboratory system.

No.	E_1 (MeV)	θ_1 (deg)	E_2 (MeV)	θ_2 (deg)	P_1P_2	ΔP_1P_2 (total)
1	6.000	37.7	5.072	50	0.269	0.009
2	7.891	37.7	6.160	50	0.267	0.007
3	7.891	45.5	5.589	50	0.380	0.009
4	7.891	45.5	6.171	50	0.325	0.012
5	7.891	45.5	6.171	50	0.320	0.009
6	7.891	45.5	6.178	50	0.361	0.012
7	9.890	36.0	6.075	50	0.227	0.012
8	9.890	37.7	5.962	50	0.245	0.012
9	9.890	45.5	5.933	50	0.330	0.011
10	9.980	45.5	6.062	50	0.301	0.009
11	9.890	60.8	5.863	50	0.503	0.015
12	9.890	60.8	6.114	50	0.441	0.015
13	9.890	60.8	6.114	50	0.474	0.017
14	9.890	75.6	6.185	50	0.521	0.016
15	9.890	85.3	5.617	50	0.485	0.023
16	9.890	85.3	5.877	50	0.484	0.020
17	9.890	100.0	5.076	50	−0.402	0.031
18	9.890	100.0	5.076	50	−0.380	0.025
19	11.156	85.3	6.213	50	+0.371	0.028
20	11.156	100.0	5.797	50	−0.386	0.029

The magnitude of the geometry corrections to P_1P_2 varied from about 0.004 to 0.03. For most of the measurements the correction was between 0.01 and 0.02.

The total uncertainty in the asymmetry P_1P_2 caused by uncertainties in the geometry-correction calculations was determined in the following manner. For each intensity ratio measured, a value of $(P_1P_2)^c$ was calculated in the normal manner except that the height of the second target and detector surface were each treated as a single segment (i.e., subdivided into one part). This is equivalent to setting both the second target and detector heights to zero. (The primary effect of the second target and detector heights is to yield values of cos$\phi^{\pm}$ different from unity[8] which are calculated with a relatively low uncertainty.) The difference between $(P_1P_2)^c$ calculated in this manner and the uncorrected value of P_1P_2 may be considered as a geometrical correction for the finite widths of targets and detectors. The uncertainty in the geometry corrections was assumed to be 60% of the finite width correction. The rms of this uncertainty and the statistical uncertainty in P_1P_2 is given as the total uncertainty in P_1P_2 in Table IV.

V. RESULTS

The polarization P_1 obtained for ^{4}He$(p,p)^4$He scattering and the information pertinent to the determina-

TABLE V. Measured values of polarization in $^4He(p,p)^4He$ scattering. Energies and angles are in the laboratory system. The thickness of the first target is ΔE_1.

No.	E_1 (MeV)	ΔE_1 (keV)	θ_1 (deg)	E_2 (MeV)	P_2^{eff}	P_1
1	6.000±0.016	72	37.7	5.072±0.025	−0.813±0.032	−0.331±0.017
2	7.891±0.013	53	37.7	6.160±0.027	−0.695±0.026	−0.385±0.018
3	7.891±0.013	49	45.5	5.589±0.033	−0.800±0.033	−0.475±0.023
4	7.891±0.013	49	45.5	6.171±0.018	−0.690±0.025	−0.471±0.024
5	7.891±0.013	49	45.5	6.171±0.018	−0.690±0.025	−0.464±0.021
6	7.891±0.013	49	45.5	6.178±0.018	−0.687±0.025	−0.524±0.026
7	9.890±0.012	48	36.0	6.075±0.077	−0.731±0.040	−0.310±0.023
8	9.890±0.012	48	37.7	5.962±0.078	−0.778±0.040	−0.315±0.022
9	9.890±0.012	41	45.5	5.933±0.068	−0.790±0.037	−0.418±0.024
10	9.890±0.012	41	45.5	6.062±0.065	−0.736±0.036	−0.409±0.023
11	9.890±0.012	33	60.8	5.863±0.047	−0.820±0.031	−0.614±0.029
12	9.890±0.012	33	60.8	6.114±0.041	−0.714±0.029	−0.617±0.033
13	9.890±0.012	33	60.8	6.114±0.041	−0.714±0.029	−0.664±0.037
14	9.890±0.012	30	75.6	6.185±0.017	−0.684±0.025	−0.761±0.036
15	9.890±0.012	47	85.3	5.617±0.016	−0.820±0.025	−0.591±0.033
16	9.890±0.012	47	85.3	5.877±0.015	−0.814±0.025	−0.595±0.030
17	9.890±0.012	48	100.0	5.076±0.015	−0.807±0.032	+0.498±0.043
18	9.890±0.012	48	100.0	5.076±0.015	−0.807±0.032	+0.471±0.037
19	11.156±0.011	43	85.3	6.213±0.022	−0.673±0.026	−0.551±0.047
20	11.156±0.011	44	100.0	5.797±0.015	−0.847±0.028	+0.455±0.036

tion of these values are presented in Table V. E_1 is the proton energy at the center of the gas target cell. The uncertainty shown for E_1 is due to the uncertainties in the determination of the beam energy and of the energy loss in the Havar foil and helium gas. The energy thickness ΔE_1 of the first target is also given in Table V. E_2 is the mean energy of protons at the center of the carbon-foil analyzing target. The uncertainty shown for E_2 is due to uncertainties in the energy losses in the Havar foil, helium gas, absorber foils, etc. P_2^{eff} is the effective polarization of the carbon-foil analyzer at E_2 and at $\theta_2=50°$ (lab). The values of P_2^{eff} were obtained using the measured values of P_2^{eff} described in Sec. III and the known values[15,18] of dP_2^{eff}/dE at $\theta_2=50°$. The uncertainty in P_2^{eff} is the rms of the statistical uncertainties in the measured values of P_2^{eff}, the uncertainty in P_2^{eff} caused by the energy uncertainty in E_2, and the uncertainty in the values of dP_2^{eff}/dE used. The uncertainty in P_1 is the total uncertainty, and was obtained by taking the rms value of the total uncertainty in P_1P_2 given in Table IV and of the uncertainty in P_2^{eff} shown in Table V.

Where more than one measurement was made at the same first scattering energy and angle, the polarizations have been averaged to give the results listed in Table VI. Also, the measurement at 9.89 MeV and 36.0° (lab) after correction for the small difference in angle has been combined with the measurement at 9.89 MeV and 37.7° (lab). To obtain the averages, each measurement of the polarization was weighted by the inverse square of the absolute error in the measurement.

A graph of the angular distribution of polarizations for $^4He(p,p)^4He$ scattering at 10 MeV is shown in Fig. 2. The results of the present measurements are indicated by triangles. The error bars shown are the total uncertainty in P_1. Also shown are the results of measurements by Brown *et al.*[8] at Wisconsin and by Rosen *et al.*[20] at Los Alamos. The height of the symbol used to show the Wisconsin results indicates the total uncertainty in the measurements. The solid line is a smooth curve drawn through the values of polarization predicted by the phase shifts determined in the present experiment.

As may be noted from the angular distribution shown in Fig. 2, the agreement between the results of the present experiment near 10 MeV and the results of the Wisconsin measurements is very good. At each angle where measurements can be compared, polarizations agree within the total uncertainty of the measurements.

The agreement between the results of the present experiment and the measurements of Rosen *et al.*[20] is also seen to be quite reasonable except at 114° (c.m.).

TABLE VI. Polarization of protons scattered elastically from ^4He. The values given here are weighted means of the measurements given in Table V. The measurements of Brown, Haeberli, and Saladin which can be compared with the present results are given in the last column.

θ_{lab} (deg)	$\theta_{c.m.}$ (deg)	$E_{p,lab}$ (MeV)	P (Present expt.)	P (Brown *et al.*)
37.7	46.5	6.00	−0.331±0.017	
		7.89	−0.385±0.018	
		9.89	−0.323±0.021	
45.5	55.9	7.89	−0.479±0.019	−0.476±0.008[a]
		9.89	−0.413±0.022	−0.444±0.009[a]
60.8	73.5	9.89	−0.626±0.030	−0.648±0.019[b]
75.6	89.7	9.89	−0.761±0.036	−0.755±0.024[b]
85.3	99.8	9.89	−0.593±0.025	
		11.16	−0.551±0.047	
100.0	114.3	9.89	+0.482±0.032	
		11.16	+0.455±0.036	

[a] These results are for $\theta_{lab}=45.8°$.
[b] These results are for $E_p=9.84$ MeV.

[20] L. Rosen, J. E. Brolley, Jr., and L. Stewart, Phys. Rev. **121**, 1423 (1961).

This difference may be reconciled in the following manner. The measurements reported by Rosen *et al.*[20] indicate a scattering acceptance angle of approximately $\pm 10°$. By using the polarization curve determined in the present experiment and the cross sections given in Ref. 9 and integrating the yield into left and right counters with $\pm 10°$ acceptance angles, a right-left intensity ratio is obtained which is in agreement with the results of Rosen *et al.*,[20] to within the total uncertainty.

The measurement of the polarization at $E_1 = 7.89$ MeV and $\theta_1 = 45.5°$ (lab) in the present experiment and the corresponding measurement in the Wisconsin experiment[8] also agree within the total uncertainty.

VI. ANALYSIS

The results of the present experiment combined with the polarization measurements by Brown *et al.*[8] and with the differential cross-section measurements by Barnard *et al.*[9] were used to make a phase-shift analysis. The analysis was carried out using the Wisconsin computer program SCRAM. A description of this program and the formula relating the phase shifts to the polarizations and differential cross sections are given in Ref. 18. The procedure was to start with a trial set of phase shifts which were modified by a gradient search routine to minimize an error function E, given by

$$E=\sum\left[\frac{\sigma_c(\theta)-\sigma_e(\theta)}{\Delta\sigma_e(\theta)}\right]^2+\sum\left[\frac{P_c(\theta)-P_e(\theta)}{\Delta P_e(\theta)}\right]^2,$$

where $\sigma_c(\theta)$ and $\sigma_e(\theta)$ are calculated and experimental cross sections, respectively, $\Delta\sigma_e$ is the uncertainty in $\sigma_e(\theta)$, $P_c(\theta)$ is the calculated polarization, etc. Only partial waves through $l=2$ were considered.

The input data consisted of 22 cross-section values and between five and seven polarization values at each energy. The uncertainties in the differential cross sections were those given in Ref. 9; 2% at 6.016, 7.967, and 9.954 MeV, and 4% at 11.157 MeV. Since the cross sections and the polarizations were measured at somewhat different energies, the polarizations were adjusted to the energy values at which the cross-section measurements had been made. These adjustments could be made quite accurately since the polarization varies and smoothly with energy and the energy differences were 70 keV or less.

TABLE VII. Phase shifts (degrees) for ^{4}He$(p,p)^4$He scattering for incident energies from 6 to 11 MeV. The uncertainties at 9.954 MeV and the error per datum point were determined in the manner described in the text. The uncertainties in the phase shifts at the other energies are similar in magnitude to those at 9.954 MeV.

E_p (MeV)	$S_{1/2}$	$P_{1/2}$	$P_{3/2}$	$D_{3/2}$	$D_{5/2}$	Error per point
6.016	−49.7	45.6	112.8	0.4	1.9	0.54
7.967	−55.0	60.7	113.9	3.8	5.2	0.63
9.954	−60.7	65.7	112.4	3.7	5.3	0.60
	+2.0	+3.5	+2.7	+1.6	+1.6	
	−1.8	−5.2	−3.4	−2.5	−2.8	
11.157	−63.2	68.2	111.9	5.4	6.5	0.95

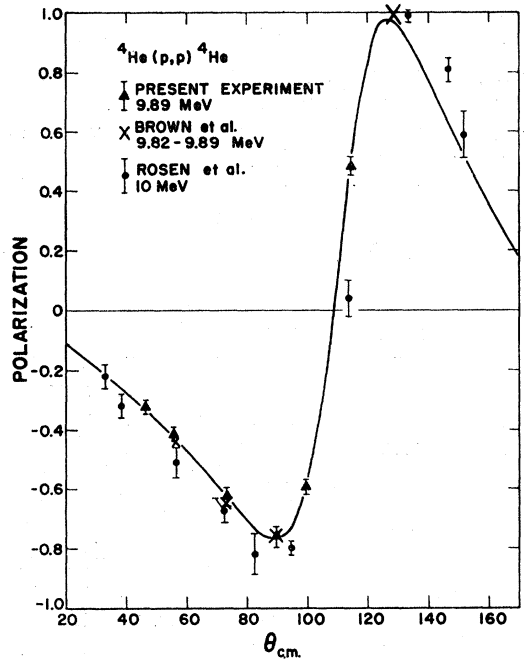

FIG. 2. Angular dependence of polarization in ^{4}He$(p,p)^4$He scattering. The smooth curve is the polarization predicted by the phase shifts determined in the present experiment. In addition to the present data, the results of Brown, Haeberli, and Saladin (see Ref. 8) and the results of Rosen *et al.* (see Ref. 20) are shown for comparison. For the data of Brown *et al.*, the height of the symbol indicates the total uncertainty in the polarization.

The results of the phase-shift search at the four energies of the present experiment are shown in Table VII. The uncertainties given for the 9.954-MeV phase shifts are discussed below. The fit to the polarization data at 9.954 MeV is shown in Fig. 2, and the cross-section fit at this same energy is shown in Fig. 3.

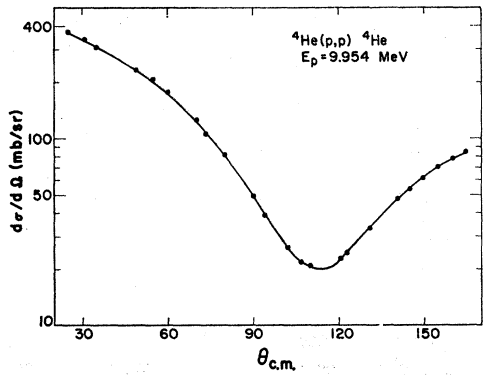

FIG. 3. Angular dependence of cross-section ^{4}He$(p,p)^4$He scattering. The smooth curve shows the cross sections predicted by the phase shifts determined in the present experiment. The circles indicate the experimental cross sections measured by Barnard *et al.* (see Ref. 9). The size of the circles indicates the total uncertainty in the measured cross sections.

To determine the necessity for d waves at 9.954 MeV, a search was made including only s and p waves. The resulting error per datum point was about 1.5. A phase-shift search was also made at 9.954 MeV, including unsplit d waves. That is, the d waves were varied in the search, but were constrained to be equal. Again, the error per datum point was about 1.5 even though the number of parameters varied increased from 3 to 4. These results provide strong evidence for split d waves at 10 MeV.

As shown in Table VII, at 9.954 MeV the phase shifts give an error per datum point of 0.6. A systematic investigation was made at this energy in order to ascertain the extent a given phase shift could be changed without increasing the error per point beyond 1.0. The procedure was as follows: The value of one phase shift was changed from that given in Table VII by an amount Δ and variation of this phase shift was then suppressed while the computer adjusted the remaining phase shifts to minimize the error function E. This procedure was repeated for several values of Δ (both positive and negative) and the resulting values of E were plotted as a function of the phase shift. Each phase shift was treated in this same manner.

The values of Δ which resulted in an error per point of 1.0 are listed as the uncertainties in Table VII. Note that strong correlations exist between the uncertainties. In particular, although the uncertainties appear to indicate that the d-wave phase shifts overlap, it was found that for every solution the $d_{5/2}$ phase shift was 1.2 to 1.8 deg larger than the $d_{3/2}$ phase shift. Thus, good fits to the data were obtained only for the $d_{5/2}$ phase shift greater than the $d_{3/2}$ phase shift, and it appears that the d-wave splitting is determined more accurately than the absolute values of the d-wave phase shifts.

In all of the above analysis the error per polarization datum point was approximately the same as the error per cross-section point.

VII. CONCLUSIONS

Polarizations in ^{4}He$(\vec{p},p)^4$He measured at four points are in excellent agreement with the measurements of Brown, Haeberli, and Saladin.[8] In order to fit the available data at 10 MeV, small positive split d waves are required with the $d_{5/2}$ phase shift 1 to 2 deg larger than the $d_{3/2}$ phase shift.

ACKNOWLEDGMENTS

The authors would like to thank Professor W. Haeberli for providing the phase-shift program and for valuable discussions. We would also like to acknowledge the assistance of Dr. G. E. Terrell and Dr. M. R. Kostoff in taking data. Computer time was kindly provided by the University of Texas Computation Center.

PHYSICAL REVIEW VOLUME 162, NUMBER 4 20 OCTOBER 1967

Upper Bounds for Errors of Expectations in the Few-Body Problem

SANFORD ARANOFF
Physics Department, Rutgers University, Newark, New Jersey
AND
JEROME K. PERCUS*
Courant Institute of Mathematical Sciences, New York University, New York, New York
(Received 1 July 1966; revised manuscript received 16 May 1967)

Exact upper bounds are established for the errors associated with approximate computations of total, kinetic, and potential energies of a few-body system. As a consequence, error bounds are also established for arbitrary coordinate functions. Reduction methods are developed to treat expectations of coordinate functions which are divergent at some spatial point, e.g., the delta function or the inverse square, or at infinity, e.g., the mean-square radius. Positronium is used as a test case to study the relative accuracy of the estimates.

1. INTRODUCTION

ONE is usually compelled to resort to approximation techniques when dealing with the few-body problem, the problem of several particles interacting via a pair potential. There are two approaches which one can follow in quantum mechanics in calculating the expectation value of some physical quantity. A direct approach is to obtain an approximate solution to the Schrödinger equation and use this to evaluate the physical quantity. This method, of course, is inefficient since it yields a great deal more information than desired. A more modest approach is to approximate the physical quantity directly, without considering the accuracy

* Supported in part by the U. S. Atomic Energy Commission under Contract No. AT(30-1)-1480.